Available online at www.sciencedirect.com
ScienceDirect
Journal of Natural Gas Chemistry 19(2010)653–659
Journal of Natural Gas Chemistry
www.elsevier.com/locate/jngc

Kinetics and product distribution studies on ruthenium-promoted cobalt/alumina Fischer-Tropsch synthesis catalyst

Ahmad Tavasoli[1*], Ali Nakhaei Pour[2], Masoumeh Ghalbi Ahangari[2]

1. School of chemistry, College of science, University of Tehran, Tehran, Iran;
2. Research Institute of Petroleum Industry, Tehran, P. O. Box 14665-137, Iran

[Manuscript received April 6, 2010; revised May 12, 2010]

Abstract

Hydrocarbon production rates and distributions on ruthenium promoted alumina supported cobalt Fischer-Tropsch synthesis (FTS) catalyst were studied by the concept of two superimposed Anderson-Schulz-Flory (ASF) distributions. The results indicated that the characterizing growth probabilities α_1 and α_2 were strongly dependent on reaction conditions. By increasing the H_2/CO partial pressure ratios and reaction temperatures, deviation from normal ASF distribution decreases and the double-α-ASF distribution changes into a straight line. Based on the concept of double-α-ASF distribution, a useful rate equation for the production of hydrocarbons under industrial reaction conditions is obtained.

Key words

Fischer-Tropsch synthesis; cobalt catalyst; ruthenium; reaction rate; products distribution

1. Introduction

The Fischer-Tropsch synthesis (FTS) offers the possibility of converting a mixture of hydrogen and carbon monoxide (synthesis gas) into clean hydrocarbons free from sulfur. Several metals, such as nickel, cobalt, ruthenium and iron, have shown to be active for this reaction [1−3]. However, only iron and cobalt based catalysts appear to be economically feasible for an industrial scale. Cobalt-catalyzed Fischer-Tropsch synthesis converts natural gas to hydrocarbon liquids with high carbon efficiency due to low water-gas shift activity of the catalyst.

Many studies on FTS were focused on the dependence of chain length distribution of hydrocarbons on catalyst types and reaction conditions [4−10]. In 1946, Herington reported that a model of stepwise addition of single-carbon units could predict the fraction of product at each carbon number [4,5]. The same formulation was rediscovered by Anderson et al. in 1951 and named the Anderson-Schulz-Flory (ASF) distribution [1,5]. In the ASF model, the formation of hydrocarbon chains was assumed as a stepwise polymerization procedure and the chain growth probability was assumed to be independent of the carbon number. However, significant deviations from the ideal ASF distribution have been observed in many studies [6−10].

Pichler et al. [11] for the first time reported the deviations of experimental results from the ASF distribution. The usual deviations of the distribution of the linear hydrocarbons are a relatively higher selectivity to methane, a relatively lower selectivity to ethane, and an increase in the chain growth probability with increasing molecular size in comparison with the ideal ASF distribution. Heat and mass-transfer limitations and hydrogenolytic cleavage of the 1-olefins in secondary reactions, are reported in the literature as possible reasons for high methane yields [12–14]. Low selectivity to ethane is attributed to another secondary reaction of the olefins, namely incorporating into the polymer by initiating a new chain [14,15]. Several different explanations about the cause of these deviations have been proposed [16−19]. Madon and Taylor [17] interpreted that this bimodal distribution by differently structured sites caused different growth probabilities. Gaube et al. [18,19] supposed that in the case of alkali-promoted catalysts not all active sites are influenced by alkali. Therefore the distribution of high growth probability was attributed to the products formed on promoted active sites while the other part of the products is formed on unpromoted sites with a similar growth probability as evaluated for the product formed on unprompoted catalysts. However, the work of Dictor and Bell [13] indicated that two chain growth probabilities existed on catalysts even the catalysts were not promoted by alkalis. Satterfield et al. [20−22] interpreted the deviations from the standard ASF distribution by the superposition of two ASF

* Corresponding author. Tel: +982161112726; Fax: +982166495291; E-mail: tavassolia@khayam.ut.ac.ir

doi:10.1016/S1003-9953(09)60133-X

distributions. They suspected the existence of two sorts of sites for the chain growth on the catalyst surface and thus proposed that each site might individually yield the ideal ASF distribution with different chain growth probabilities. Patzlaff et al. [23] indicated that chain length distributions of products obtained on cobalt catalysts are slightly modified by secondary chain growth of re-adsorbed alkenes and hydrogenolysis of hydrocarbons.

In our previous works [24,25] the reaction rate and products distribution of iron catalyst were studied. In this research the hydrocarbon production rates and product distributions of ruthenium promoted alumina supported cobalt Fischer-Tropsch synthesis catalyst were studied, using a modified Anderson-Schulz-Flory (ASF) distribution with two chain growth probabilities.

2. Data analysis

As discussed above, the hydrocarbon products of the Fischer-Tropsch synthesis are generally taken to follow the ASF distribution. For carbon number i, the mole fraction of product x_i determined by a single chain growth probability α, is given by:

$$x_i = (1-\alpha)\alpha^{i-1} \tag{1}$$

In this work the carbon number distribution of Fischer-Tropsch products on alumina supported cobalt catalyst was studied by a modified Anderson-Schulz-Flory distribution with two chain growth probabilities. This method was proposed by Donnelly et al. [22] and is used to characterize the carbon number distribution of Fischer-Tropsch synthesis where independent ASF distributions with different chain growth probabilities are superimposed.

$$x_i = A\alpha_1^{i-1} + B\alpha_2^{i-1} \tag{2}$$

Instead, we note that at the break point on ASF diagram, the contributions of each term in Equation (2) are equal.

$$A\alpha_1^{i-1} = B\alpha_2^{i-1} \quad i = \zeta \tag{3}$$

At break point, i illustrates as ζ and is necessarily not an integral carbon number. In this model A and B are not assumed to correspond directly to the fractions of products produced from α_1 and α_2, respectively. Instead the sum of the mole fractions over all carbon numbers is unity:

$$\sum_{i=1} x_i = \sum_{i=1} [A\alpha_1^{(i-1)} + B\alpha_2^{(i-1)}] = 1 \tag{4}$$

Methane and ethane do not obey the ASF equation and after removing C_1 and C_2 products to fit theoretical distributions to data leads to:

$$\sum_{i=3} x_i = \sum_{i=1} [A\alpha_1^{(i-1)} + B\alpha_2^{(i-1)}] - A(1+\alpha_1) - B(1+\alpha_2) = 1 - x_1^{\exp} - x_2^{\exp} \tag{5}$$

Therefore, the determination of growth probabilities of the bimodal ASF distribution is based on hydrocarbons with carbon numbers $i>2$. The bimodal distribution is characterized by two growth probabilities (α_1 and α_2) and the point of intersection ξ of both ASF distributions. The mathematical procedure given by Donnelly et al. [22] as follows:

$$A = (1 - x_1^{\exp} - x_2^{\exp}) \left[\frac{\alpha_1^2}{1-\alpha_1} + \left(\frac{\alpha_1}{\alpha_2}\right)^{\xi-1} \cdot \left(\frac{\alpha_2^2}{1-\alpha_2}\right) \right]^{-1} \tag{6}$$

and finally at

$$\frac{x_i}{1 - x_1^{\exp} - x_2^{\exp}} = \left[\alpha_1^{i-1} + \left(\frac{\alpha_1}{\alpha_2}\right)^{\xi-1} \cdot \alpha_2^{i-1} \right] \cdot \left[\frac{\alpha_1^2}{1-\alpha_1} + \left(\frac{\alpha_1}{\alpha_2}\right)^{\xi-1} \cdot \left(\frac{\alpha_2^2}{1-\alpha_2}\right) \right]^{-1} \tag{7}$$

The three parameters α_1, α_2 and ξ are evaluated by minimizing the least squares:

$$= \sum_{i=3}^{I} \left(\ln x_1 - \ln x_l^{\exp}\right)^2 = \min \tag{8}$$

in which I is the upper limit of experimental data. The advantage of Donnelly method is its independence of this upper limit I. However, the intersection point ξ is a formal parameter without any physicochemical relevance.

3. Kinetics

The hydrocarbon production rates on FTS catalysts have been correlated empirically by Dictor and Bell [13] as power-law kinetics:

$$R_{C_i} = k_i P_{H_2}^a P_{CO}^b \tag{9}$$

The formation rates of hydrocarbons increased with increasing the H_2 partial pressure. Assuming ASF for the distribution of the small-chain hydrocarbons, the chain growth probability appeared to increase with increasing CO pressure and decreasing H_2 pressure. The hydrocarbon production rates could be calculated using [13,26]:

$$R_{C_i} = R_{C_1}\alpha^{i-1} \tag{10}$$

where, R_{C_i} is the molar rate of hydrocarbons production with i carbon atoms and R_1 is the apparent rate of synthesis for $i = 1$ but does not necessarily represent the rate of methane formation. In this study we consider C_3 production rate as R_1 and α_1 as α for $i = 4$ to 13 and C_{13} production rate as R_1 using the α_2 for $i = 14$ to 32, and compared calculated hydrocarbons production with experimental results. The dependence of R_{Ci} on H_2 and CO partial pressures can now be expressed through R_1 and α. From its definition [13,26,27], we can relate α to the ratio of the rates of chain propagation r_p and chain termination r_t.

$$\frac{1-\alpha}{\alpha} = \frac{r_p}{r_t} \tag{11}$$

Based on Dictor and Bell [13] results we presume that the right-hand side of Equation (11) will be a function of the

partial pressures of H_2 and CO and temperature. The relative value of the reaction activation energy barriers for chain growth and termination steps in the FTS reaction, can be determined using Arrhenius theory for evaluation of temperature dependency of α based on Yang et al. method [27]:

$$r_p = A_p \exp\left(\frac{-E_p}{RT}\right) \quad (12)$$

$$r_t = A_t \exp\left(\frac{-E_t}{RT}\right) \quad (13)$$

E_p and E_t are activation energies for propagation and termination reactions, respectively. By introducing Equations (12) and (13) into Equation (11):

$$\frac{1-\alpha}{\alpha} = \frac{A_t}{A_p} \exp\left(\frac{E_p - E_t}{RT}\right) \quad (14)$$

Equation (14) can be rewritten as:

$$\ln\frac{1-\alpha}{\alpha} = \ln\frac{A_t}{A_p} + \left(\frac{E_p - E_t}{RT}\right) \quad (15)$$

Equation (15) predicts a linear plot of ln[(1-α)/α] versus 1/T with the slope of (E_p–E_t)/R and the intercept of ln A_t/A_p.

4. Experimental

4.1. Catalyst preparation

Ruthenium promoted (Ru/Co = 0.010 by weight) cobalt catalysts were prepared with 30 wt% cobalt on γ-alumina support as described previously [28]. The support was first calcined at 500 °C for 10 h. The catalyst was prepared by sequential aqueous impregnation of the support with the appropriate solution of the cobalt nitrate ($Co(NO_3)_2{\cdot}6H_2O$, 99.0%, Merck) and ruthenium (III) nitrosylnitrate ($Ru(NO)(NO_3)_3$). After each step, the catalyst sample was dried at 120 °C and calcined at 450 °C for 3.5 h.

4.2. Catalytic performance

Catalysts were tested using a fixed-bed micro-reactor. A detailed description of the experimental setup and procedures has been provided in our previous work [28]. Typically, 1.5 g of the catalyst was charged into a "1/4" stainless steel tubular reactor. The reactor was placed in a molten salt bath with a stirrer to ensure a uniform temperature along the catalyst bed. The temperature of the bath was controlled via a PID temperature controller. Separate mass flow controllers (Brooks 5850) were used to add H_2 and CO at the desired rate to a mixing vessel that was preceded by a lead oxide-alumina containing vessel to remove carbonyls before entering the reactor. Prior to the activity tests, the temperature was raised to 400 °C with a heating rate of 1 °C/min and the catalysts was reduced in a flow of H_2 for 12 h.

For kinetic studies, a stabilization period of more than 100 h was used to ensure that the stable catalytic reactions were established (results not shown here). The experimental conditions were varied as follows: temperatures from 210 °C to 240 °C, P_{H_2}/P_{CO} feed ratio from 0.5 to 2.0, pressure 25 bar and space velocity 1120 h^{-1}. At regular intervals, the standard experiment was repeated to determine possible deactivation effects of the catalysts. Kinetic samples were cumulatively collected during a typical period of 10 –16 h. For each operation condition, it took at least 10 h to ensure the steady state behavior of the catalyst after a change of the reaction conditions.

The products were analyzed by three gas chromatographs. A Shimadzu 4C gas chromatograph equipped with two sequentially connected packed columns: Porapak Q and Molecular Sieve 5A, and a thermal conductivity detector (TCD) with argon which was used as a carrier gas for hydrogen analysis. A Varian CP 3800 with a chromosorb column and a thermal conductivity detector (TCD) were used for CO, CO_2, CH_4, and other non-condensable gases. A Varian CP 3800 with a Petrocol^{Tm} DH100 fused silica capillary column and a flame ionization detector (FID) were used for organic liquid products so that a complete product distribution could be provided.

5. Results

5.1. Product distribution studies

The chain length distribution of Fischer-Tropsch products formed on the cobalt catalysts can be well characterized by a double-ASF-distribution. Our results focus on the effect of process variables on carbon number distribution. In all cases, a double-α-ASF distribution was required to fit the data. Chain length distributions were calculated using a method described by Donnelly et al. [22] as described in previous section. Typically we used the entire range from C_3 to C_{32} to calculate α_1 and α_2. The chain length distributions and growth probabilities α_1 and α_2 depend mainly on reaction conditions of the FT synthesis.

The effects of H_2/CO partial pressure ratios on chain length distribution of catalyst at 220 °C, 25 bars, and space velocity 1120 h^{-1} are given in Figure 1. This Figure shows that the average carbon number of products is decreased with

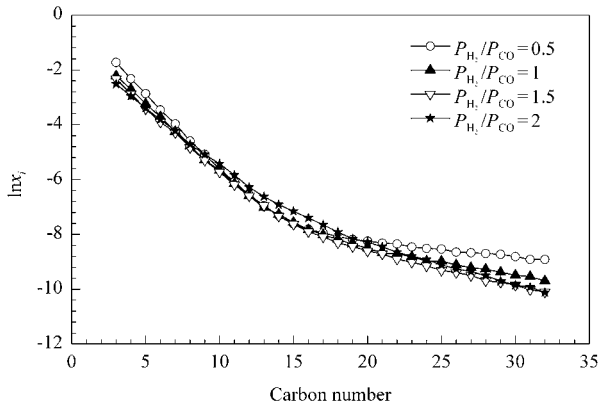

Figure 1. The effects of H_2/CO partial pressure ratios in feed on chain length product distribution of Ru-Co/alumina catalyst. Reaction conditions: 220 °C, total pressure 25 bar, space velocity 1120 h^{-1}

increasing the partial pressure of H_2. As shown in Figure 1, with increasing the H_2/CO partial pressure ratios, deviation from normal ASF distribution decreases and a double-α-ASF distribution changes into a straight line.

Chain length product distributions at different reaction temperatures are given in Figure 2. This Figure shows that with increasing the reaction temperature, average carbon number of products decreases and breakdown in ASF distribution shifts to low carbon numbers.

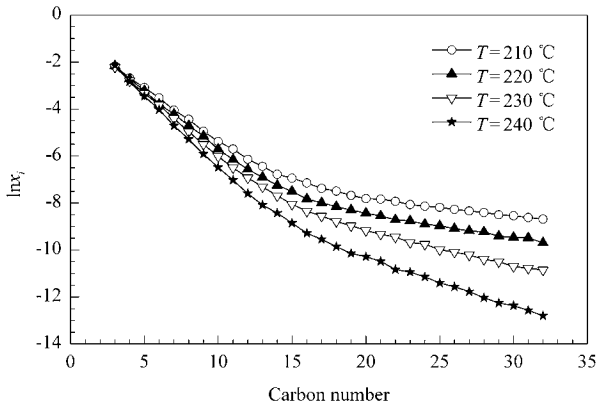

Figure 2. Effects of reaction temperatures on Ru-Co/Alumina catalyst chain length product distributions. Reaction conditions: $P_{H_2}/P_{CO} = 2$, pressure 25 bar, space velocity 1120 h^{-1}

The characterizing growth probabilities α_1 and α_2 are listed in Table 1. Both probabilities depend on reaction conditions. Table 1 illustrates that the value of α_1 slightly increased while the growth probability α_2 slightly decreased as the H_2/CO partial pressures ratio increased. Also the values of α_1 and α_2 slightly decreased as the FT reaction temperature increased. A similar result is obtained by Donnelly [29] and Dictor [13]. These results indicated that by increasing the reaction temperature, values of α_1 and α_2 approach to each other and deviation from ASF distribution decreases so a double-α-ASF distribution changes into a straight line at high temperatures.

Table 1. Chain growth probabilities and kinetics parameters of Ru-Co/Alumina catalyst in FTS reactions

		α_1	α_2
T (°C)	210	0.62	0.93
	220	0.59	0.91
	230	0.57	0.87
	240	0.53	0.82
P_{H_2}/P_{CO}	0.5	0.57	0.95
	1.0	0.59	0.91
	1.5	0.60	0.89
	2.0	0.63	0.87
A_t/A_p		22	3.9×10^3
E_p–E_t (kJ/mol)		−16.2	−49.2

5.2. Kinetics studies

Figure 3 shows that the experimentally observed values of chain growth probabilities α_1 and α_2 produce a straight line when $(1–\alpha)/\alpha$ is plotted versus P_{H_2}/P_{CO}. The equations of the chain growth probabilities α_1 and α_2 as function of P_{H_2}/P_{CO} are derived from straight line parameters as:

$$\frac{(1-\alpha_1)}{\alpha_1} = 0.81 - 0.11\frac{P_{H_2}}{P_{CO}} \quad (16)$$

$$\frac{(1-\alpha_2)}{\alpha_2} = 0.03 + 0.06\frac{P_{H_2}}{P_{CO}} \quad (17)$$

These equations show that in contrast to the α_2, α_1 is strongly dependent on the H_2 and CO partial pressures. The molar rates of production for C_3 and C_{14} hydrocarbons as a function of P_{H_2} and P_{CO} in the form of power-law rate expressions, by fitting the experimentally results were obtained as:

$$R_{C_3} = 0.03P_{H_2}^{0.09}P_{CO}^{-1} \quad (18)$$

$$R_{C_{14}} = 2\times10^{-6}P_{H_2}^{2}P_{CO}^{-1} \quad (19)$$

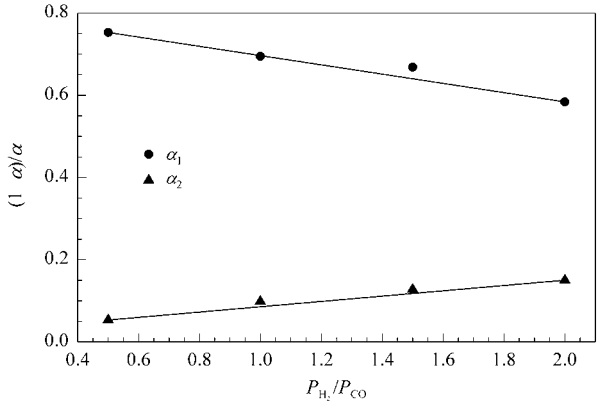

Figure 3. Empirical correlation between growth probabilities α_1 and α_2 and reactant partial pressures for Ru-Co/alumina catalyst. Reaction conditions: 220 °C, total pressure 25 bar, and space velocity 1120 h^{-1}

Based on Dictor and Bell methods for hydrocarbons production rates (Equation 10) [13], by introducing Eqations (20) and (21) into equations with chain growth probabilities α_1 and α_2 as function of P_{H_2}/P_{CO} (Equations 16 and 17), the hydrocarbon production rates of $i = 4$ to 13 and $i = 15$ to 32, for Ru-Co/Alumina catalyst were obtained as:

$$R_{C_i} = \frac{0.03P_{H_2}^{0.09}P_{CO}^{-1}}{\left(1.81 - 0.11\dfrac{P_{H_2}}{P_{CO}}\right)^{i-1}} \quad \text{For } i = 4 \text{ to } 13 \quad (20)$$

$$R_{C_i} = \frac{2\times10^{-6}P_{H_2}^{2}P_{CO}^{-1}}{\left(1.03 - 0.06\dfrac{P_{H_2}}{P_{CO}}\right)^{i-1}} \quad \text{For } i = 15 \text{ to } 32 \quad (21)$$

The observed H_2 dependency of light hydrocarbon ($i = 4$ to 13) production was 0.09 and increased with increasing carbon number to 2 for heavy hydrocarbon ($i = 15$ to 32). The observed CO dependency was -1 for light hydrocarbons ($i = 4$ to 13) and does not changed with carbon number.

The representation of the data in this fashion and the comparison of the results with experimental data are shown in Figures 4 and 5 . These Figures show that the experimental

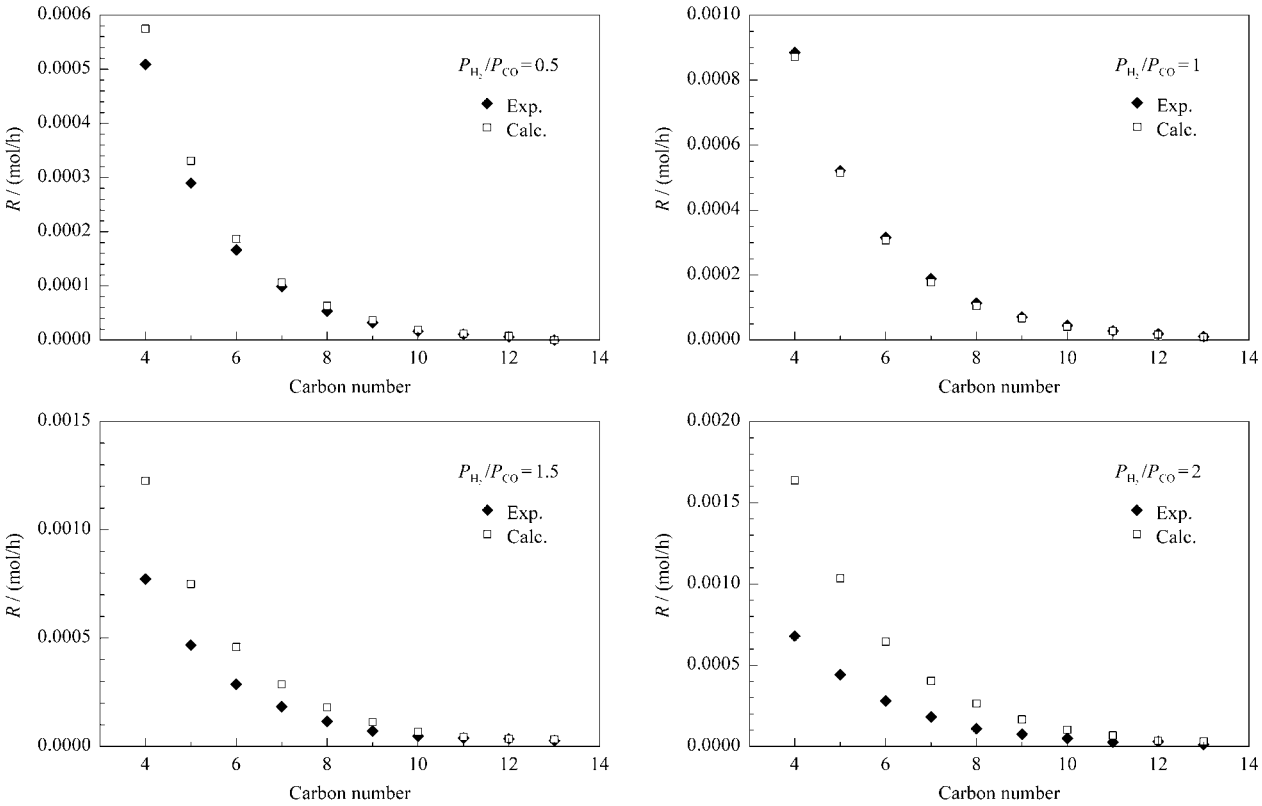

Figure 4. Comparison between experimental and calculated results by considering chain length probability α_1 for $i = 4$ to 13 carbon product formation rates. Reaction conditions: 220 °C, pressure 25 bar, space velocity 1120 h^{-1}

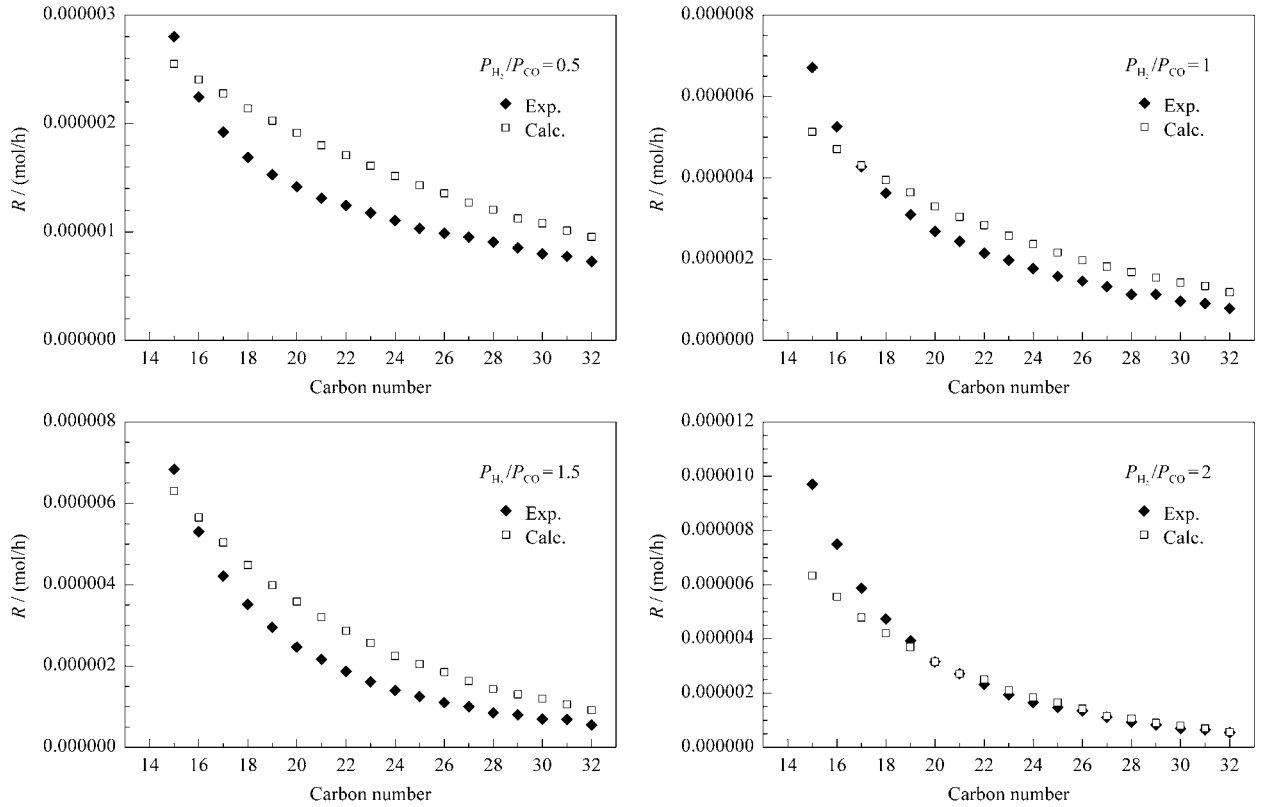

Figure 5. Comparison between experimental and calculated results by considering chain length probability α_2 for $i = 15$ to 32 carbon product formation rates. Reaction conditions: 220 °C, pressure 25 bar, space velocity 1120 h^{-1}

data are almost confirmed by the calculated results. The curvature seen in the lines is a direct result of the dependence of α on the reactant partial pressures and the dependence of R_{Ci} on α^{i-1}. Since the dependence of α on H_2 and CO partial pressures for α_2 is much weaker than α_1, the kinetics for C_{15}–C_{32} hydrocarbon synthesis is dominated by the power-law dependence of $R_{C_{14}}$. This explains why the small change occurs in slope with the increase of carbon number for high hydrocarbons.

The plots of ln ((1–α)/α) versus 1/T for evaluating temperature dependency of chain growth probabilities α_1 and α_2, are shown in Figure 6. This figure shows that by increasing the reaction temperature, the chain growth probabilities α_1 and α_2 are decreased. From the slopes and the intercepts of the straight lines in Figure 6, the difference between activation energies for propagation and termination reactions (E_p–E_t) and the ratio A_t/A_p are obtained (listed in Table 1). As shown in Table 1, the reaction activation barrier for chain growth is lower than that for chain termination for both α_1 and α_2 growth probabilities and E_p–E_t difference for α_1 is lower than that for α_2. This may be due to the fact that the mechanisms of growth probabilities for α_1 and α_2 are different at chain growth step and termination step.

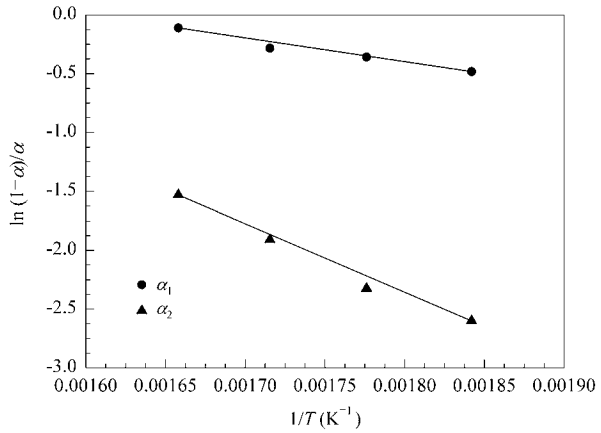

Figure 6. Empirical correlation between growth probabilities α_1 and α_2 and reciprocal reaction temperatures for Ru-Co/alumina catalyst. Reaction conditions: P_{H_2}/P_{CO} = 2, pressure 25 bar, space velocity 1120 h^{-1}

6. Discussion

The hydrocarbon production rates and carbon number distribution of ruthenium promoted cobalt/alumina catalysts in Fischer-Tropsch syntheses were studied. The concept of Anderson-Schulz-Flory (ASF) distribution with two chain growth probabilities was used to evaluate experimental data. This method proposed by Donnelly et al. [22] was used to characterize the carbon number distribution of Fischer-Tropsch synthesis where independent ASF distributions with different chain growth probabilities are superimposed. The carbon number distribution of the products formed on cobalt catalysts can be represented by two ASF distributions with a slope change on C_{14} hydrocarbon as shown in Figures 1 and 2. The origin of the break is not established clearly. König [18] and Satterfield [16] proposed that the two branches observed with potassium promoted catalysts are resulted from the synthesis performing over two groups of active sites with different promotion level. This interpretation may not be the only one since Huff [6] have shown that some unpromoted catalysts can also produce ASF plots, which consist of two branches. Dictor et al. [13] suggested that deviations from uniform ASF distributions might result from the chemistry of the Fischer-Tropsch synthesis. The most accepted mechanism is CH_2 insertion, which leads to conclude the carbide theory of Fischer-Tropsch [29]. In this mechanism, chain termination occurs mainly with elimination of β-hydrogen and desorption of 1-alkenes as primary products. In the following reactions, readsorbed 1-alkenes are hydrogenated to form intermediates for surface intermediate chain growth with C_1 surface species. These C_1 species having various hydrogenation degrees are the CO, HCO, HCOH, CH and CH_2.

Patzlaff et al. [23] suggested that the degree of hydrogenation of monomers for the products described with α_1 is higher than those with α_2. Therefore, CH_2 is assumed as C_1 intermediate and attributed to the distribution of growth probability α_1. Obviously, hydrocarbon chain growth probability α_2 are built up due to monomers except CH_2 species with low degree of hydrogenation. Higher hydrogen concentration on catalyst surface enhanced the concentration of monomers with higher degree of hydrogenation and increased the α_1 chain growth probability. The products with high carbon number and related chain growth probability (α_2) are decreased by increasing the H_2 partial pressures. Figure 1 shows that by increasing the H_2/CO ratio, the average carbon number of the products, decreased. Table 1 shows the growth probabilities α_1 and α_2 of these distributions. As shown in this Table, α_1 is increased, while growth probability α_2 is decreased by increasing the H_2/CO partial pressure ratio. Although at high hydrogen partial pressures, α_1 and α_2 are close together and the point of breakdown on the ASF distribution shifts to low molecular weight hydrocarbons.

Table 1 and Figure 2 exhibited that by increasing the FTS reaction temperatures, carbon number of the products and values of α_1 and α_2 are slightly decreased. This fact may be related to high mobility of hydrocarbon chains on the surface of catalysts at the high temperature. The vibrations of those growing long chains on catalyst surface are increased by raising the reaction temperature, and cause the desorption to become quick. As a result, average carbon number and both chain growth probabilities α_1 and α_2 decrease.

As shown in Table 1, the reaction activation barrier of the chain growth is lower than the chain termination for both α_1 and α_2 chain growth probabilities and E_p–E_t difference for α_1 is lower than α_2 chain growth probability. This may be due to the fact that the mechanisms of chain growth probabilities α_1 and α_2 are conflicting with the barriers of the chain growth and termination.

7. Conclusions

Chain length distributions of Fischer-Tropsch products on ruthenium-promoted cobalt/alumina catalyst were studied by the concept of two superimposed Anderson-Schulz-Flory (ASF) distributions. These results indicated that with increasing the H_2/CO partial pressure ratios and reaction temperatures, deviation from normal ASF distribution decreases and a double-α-ASF distribution changes into a straight line. Also with introduction of a double-α-ASF distribution, a useful power-law hydrocarbon production rate equation can be obtained.

References

[1] Anderson R B. The Fischer-Tropsch synthesis. New York: Academic Press, 1984
[2] Dry M E. In: Anderson Jr, Boudart M ed. Catalysis Science and Technology 1. Springer-Verlag. 1981, Vol.1, p159
[3] Bartholomew C H. Recent Developments in Fischer-Tropsch Catalysis, New Trends in CO Activation. In: Studies in Surface Science and Catalysis, No. 64. Elsevier, 1991
[4] Herington E F G. *Chem Ind* (*London)*, 1946, 65: 346
[5] Friedel R A, Anderson R B. *J Am Chem Soc*, 1950, 72(3): 1212
[6] Huff J G A, Satterfield C N. *Ind Eng Chem Process Des Dev*, 1985, 24(4): 986
[7] Wojciechowski B W. *Catal Rev Sci Eng*, 1988, 30(4), 629
[8] Novak S, Madon R J, Suhl H. *J Chem Phys*, 1981, 74(11): 6083
[9] Novak S, Madon R J, Suhl H. *J Catal*, 1982, 77(1): 141
[10] Iglesia E, Soled S L, Baumgartner J E, Reyes S C. *J Catal*, 1995, 153(1): 108
[11] Pichler H, Schultz H, Elstner M. *Brennst Chem*, 1967, 48: 78
[12] Dry M E. *J Mol Catal*, 1982, 17(2-3): 133
[13] Dictor R A, Bell A T. *J Catal*, 1986, 97(1): 121
[14] Puskas I, Hurlbut R S. *Catal Today*, 2003, 84(1-2): 99
[15] Puskas I, Hurlbut R S, Pauls R E. *J Catal*, 1993, 139(2): 591
[16] Satterfield C N, Huff G A. *J Catal*, 1982, 73(1): 187
[17] Madon R J, Taylor W F. *J Catal*, 1981, 69(1): 32
[18] König L, Gaube J. *Chem Ing Tech*, 1983, 55(1): 14
[19] Schliebs B, Gaube J. *Bunsenges Ber Phys Chem*, 1985, 89: 68
[20] Satterfield C N, Huff Jr G A, Longwell J P. *Ind Eng Chem Process Des Dev*, 1982, 21(3): 465
[21] Huff J G A, Satterfield C N. *J Catal*, 1984, 85(2): 370
[22] Donnelly T J, Yates I C, Satterfield C N. *Energy Fules*, 1988, 2(6): 734
[23] Patzlaff J, Liu Y, Graffmann C, Gaube J. *Appl Catal A*, 1999, 186(1-2): 109
[24] Pour A N, Zamani Y, Tavasoli A, Shahri S M K, Taheri S A. *Fuel*, 2008, 87(10-11): 2004
[25] Pour A N, Shahri S M K, Bozorgzadeh H R, Zamani Y, Tavasoli A, Marvast M A. *Appl Catal A*, 2008, 348(2): 201
[26] Van Der Laan G P, Beenackers A A C M. *Catal Rev Sci Eng*, 1999, 41(3-4): 255
[27] Yang Y, Pen S, Zhong B, Wang Q. *Catal Lett*, 1993, 19(1): 93
[28] Tavasoli A, Nakhaeipour A, Sadaghiani K. *Fuel Process Technol*, 2007, 88(5): 461
[29] Donnelly T J, Satterfield C N. *Appl Catal*, 1989, 52(1): 93
[30] Fischer F, Tropsch H. *Brennst Chem*, 1926, 7: 97